

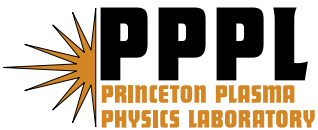
PPPL-4187

PPPL-4187

**Reference Lithium Deposition
on NSTX Plasma Facing Components
by LITER-1 Evaporator**

L.E. Zakharov, H.W. Kugel, A.L. Roquemore,
and C.H. Skinner

November 2006



Princeton Plasma Physics Laboratory

Report Disclaimers

Full Legal Disclaimer

This report was prepared as an account of work sponsored by an agency of the United States Government. Neither the United States Government nor any agency thereof, nor any of their employees, nor any of their contractors, subcontractors or their employees, makes any warranty, express or implied, or assumes any legal liability or responsibility for the accuracy, completeness, or any third party's use or the results of such use of any information, apparatus, product, or process disclosed, or represents that its use would not infringe privately owned rights. Reference herein to any specific commercial product, process, or service by trade name, trademark, manufacturer, or otherwise, does not necessarily constitute or imply its endorsement, recommendation, or favoring by the United States Government or any agency thereof or its contractors or subcontractors. The views and opinions of authors expressed herein do not necessarily state or reflect those of the United States Government or any agency thereof.

Trademark Disclaimer

Reference herein to any specific commercial product, process, or service by trade name, trademark, manufacturer, or otherwise, does not necessarily constitute or imply its endorsement, recommendation, or favoring by the United States Government or any agency thereof or its contractors or subcontractors.

PPPL Report Availability

Princeton Plasma Physics Laboratory:

http://www.pppl.gov/pub_report/

Office of Scientific and Technical Information (OSTI):

<http://www.osti.gov/bridge>

U.S. Department of Energy:

U.S. Department of Energy
Office of Scientific and Technical Information
P.O. Box 62
Oak Ridge, TN 37831-0062
Telephone: (865) 576-8401
Fax: (865) 576-5728
E-mail: reports@adonis.osti.gov

Reference lithium deposition on NSTX plasma facing components by LITER-1 evaporator

L.E. Zakharov, H.W. Kugel, A.L. Roquemore, C.H. Skinner

September 15, 2006

Abstract

The calculation by Cbebm code of lithium deposition from the LITER-1 lithium evaporator on the surface of the graphite tiles of NSTX during 2006 campaign is presented. The numerical model represents a collisionless gas model which assumes re-evaporation of the Li molecules after their collision with the wall. The data can serve as a reference Li deposition distribution, which would be established in a perfectly clean vacuum vessel.

For easy navigation the enumeration in the Table of Contents, and the “(to ToC)” right after the section names are the forward and backward hyperlinks between Table of Contents and the beginning of sections.

Contents

1	Introduction	1
2	Plasma facing components inside NSTX vacuum vessel	2
3	Shadow region on the PFC	6
4	Numerical data for deposition monitors, coupons, and test tiles	8
5	Appendix	9

[1](#) [Introduction](#) *(to ToC)*

In 2006, NSTX conducted several experiments with intense lithium deposition on its ATJ graphite plasma facing components from an evaporator “LITER-1”[1] situated in the upper part of the vacuum chamber. Although it had a noticeable positive effect on the plasma discharges following the evaporation, an expected high rate of pumping of plasma particles by the lithium coating was not observed. The interaction of the lithium coating, established gradually on the graphite plates during the evaporation, with residual oxygen, water vapor, carbon sputtered off the plates could be the potential causes of passivation of the lithium layer. Also consumption and redeposition of lithium by the plasma itself can affect the efficiency of plasma pumping by the lithium.

While special studies of graphite tile surfaces are under way, it is important to have a reference Li deposition distribution for an idealized situation, when only direct deposition from the evaporator is present. Upto the temperature of $\simeq 650^\circ$ C, the lithium vapor inside LITER-1 is collisionless. In this case the angular diagram of evaporation, calculated by Cbebm code, corresponds to the rare gas Knudsen model and does not depend on temperature of the evaporator. This makes calculations of the deposition rate relative to one of the quartz crystal microbalance deposition monitors[2] (named QMB-HL) relevant to the post-campaign analysis.

We illustrate here the 3-D model of plasma facing components of NSTX and provide the numerical data on relative (to QMB-HL monitor) lithium deposition on a set of coupons and test tiles. The numerical model of evaporator itself and the code developed (Cbebm) will be presented elsewhere.

2 Plasma facing components inside NSTX vacuum vessel *(to ToC)*

A fish eye photo picture of the interior of NSTX vacuum chamber is given in Fig.1.

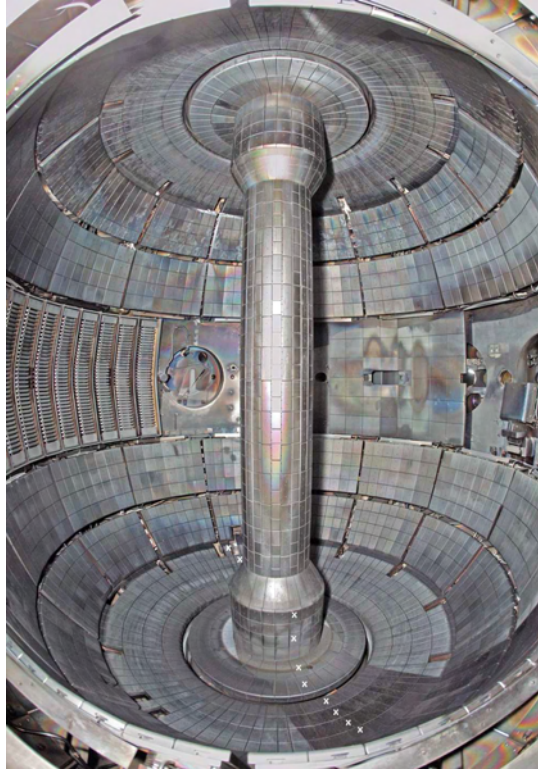
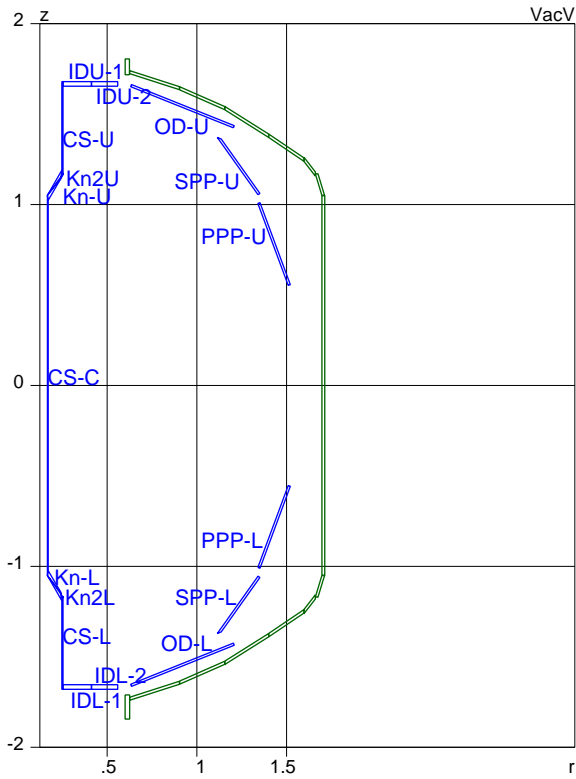


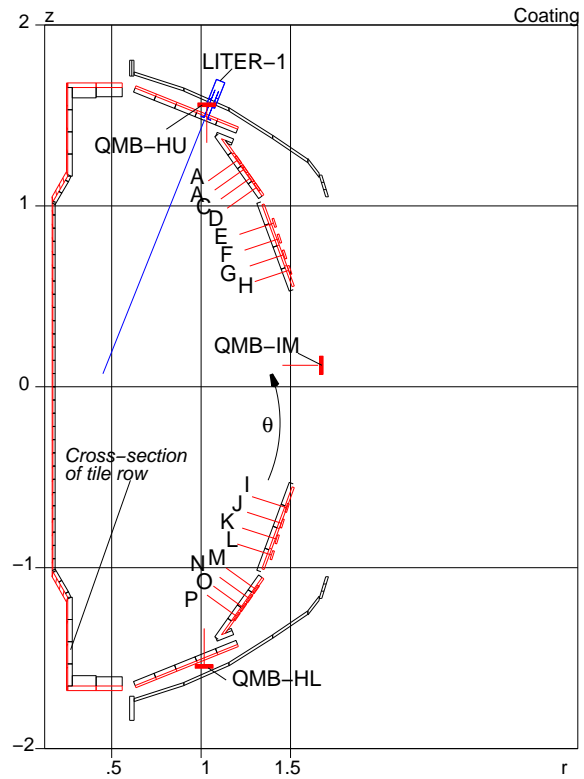
Fig.1 NSTX interior with graphite plasma facing components

The central stack, lower and upper divertor area have a continuous coverage by graphite tiles. On the sides the vacuum chamber there are 4 sets of stabilizing plates, each consisting from 12 sectors. The gaps between sectors (or Bays) are alphabetically labeled in a clockwise direction (when looking from the top) from 'A' to 'L'. White crosses in Fig.1 show some test tiles taken out for the surface analysis.

Note, that in calculations presented in this paper, the mathematical, counter clockwise direction of the azimuth φ is adopted with the origin $\varphi = 0$ at the middle of 'LA' sector.



Names of PFC elements (blue color)



Quartz MicroBalance monitors and Si witness coupons (A-P). Red lines are normal to active surfaces of monitors and coupons.

Fig.2

Fig.2 shows the poloidal cross-section of Plasma Facing Components (PFC) and the vacuum vessel together with the given names of the components, the names of Si witness coupons for collecting overall lithium deposition, and names of the Quartz MicroBalance monitors (QMB-**) used for recording the time history of deposition, where two letters in their names after '-' refer to the Bay label and position (Lower, Middle, and Upper). One of them, i.e. QMB-HL is used in calculations as the normalization signal.

Also, the cross-sections of the tile rows (black boxes on the top of red mounting plates) can be distinguished on the right side of Fig.2. In the Table 2 of Appendix the rows (within each multi-row PFC) are enumerated in the direction of the poloidal angle θ shown on Fig.2.

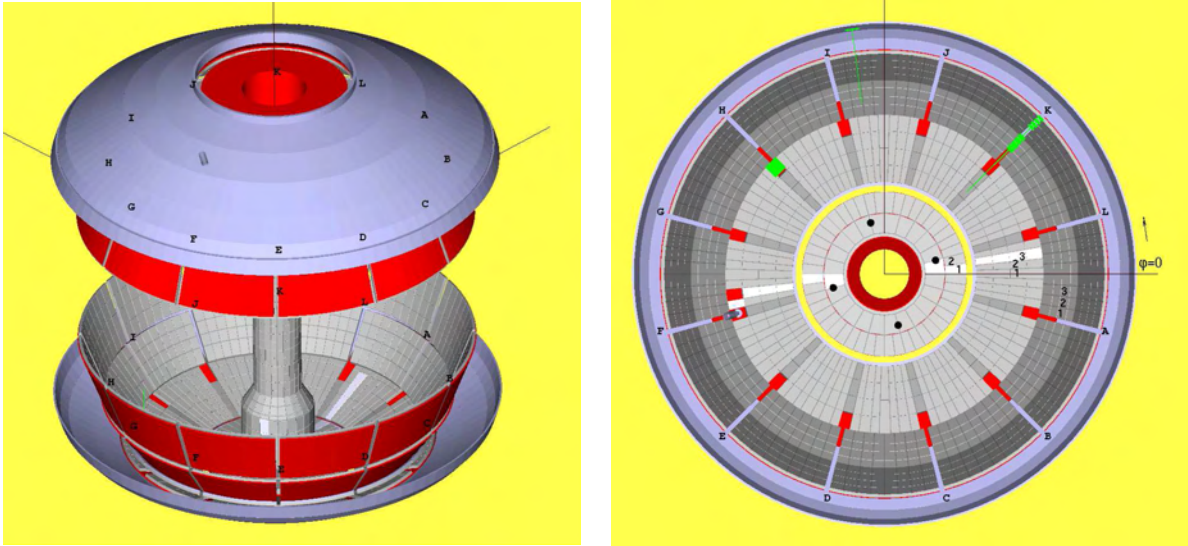


Fig.3. 3-D numerical model of NSTX PFCs for Bays A to L. Carbon tiles (gray), test tiles (looking white), and diagnostic viewport gaps (red) in the lower divertor of NSTX. The horizontal line is $\varphi = 0$ azimuth (between Bays A and L counted counter clockwise)

Fig.3 shows the numerical 3-D representation of the vacuum vessel and its ATJ graphite tiles. Shown in red at the lower outer divertor are the diagnostic viewports at each Bay. The light gray tiles are the locations at Bays F and L where tiles were removed after the end of the campaign for off-site surface analysis of lithium interaction with the graphite. The darker gray columns on the outer divertor tiles have been artificially distinguished to trace the gaps in the passive stabilizing plates associated with enumeration of Bays A-L.

Characteristic examples of enumeration of tiles in each row (used in the Appendix table 2) are shown on the right Fig.3. For passive plates (PPP-L,U, SPP-L,U) each sector has its local enumeration.

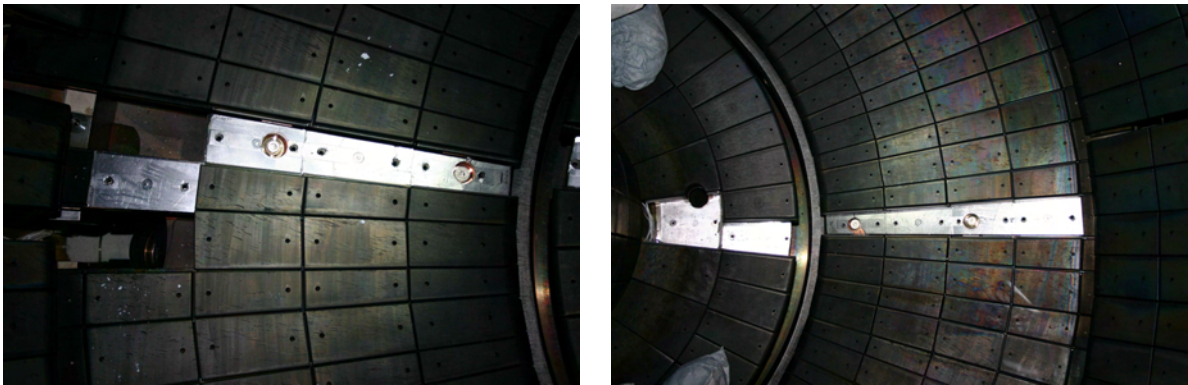


Fig.4. Photographs of the lower divertor at Bays F and L with the test tiles removed.

Fig.4 shows photographs of the Bay F and Bay L regions with the test tiles removed after the end of the campaign. The darker rectangles are the graphite tiles and the shiny metallic regions are the backing plates for the removed tiles.

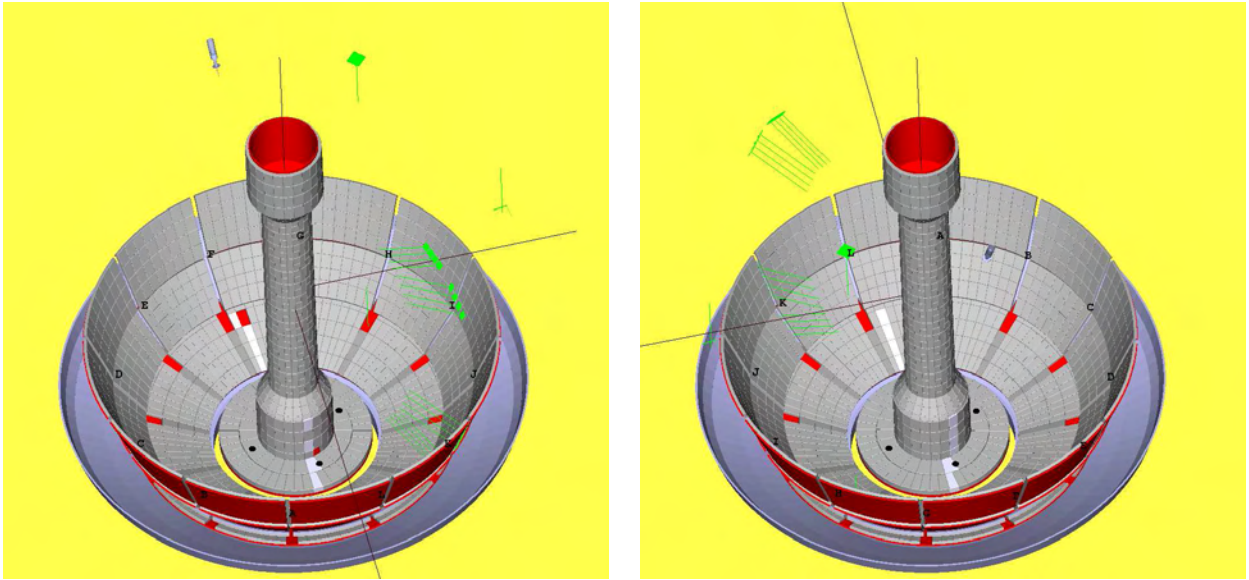


Fig.5 Test tiles at the bottom part of the central stack on numerical model

Fig.5 shows test tiles on the shadow (Bay-L) and front (Bay-F) sides of the lower part of the central stack and their numerical model.



Test tiles in vicinity of the lower Bay-L



Test tiles in vicinity of the lower Bay-F

Fig.6 Photo picture of the test tiles taken from the bottom part of the central stack.

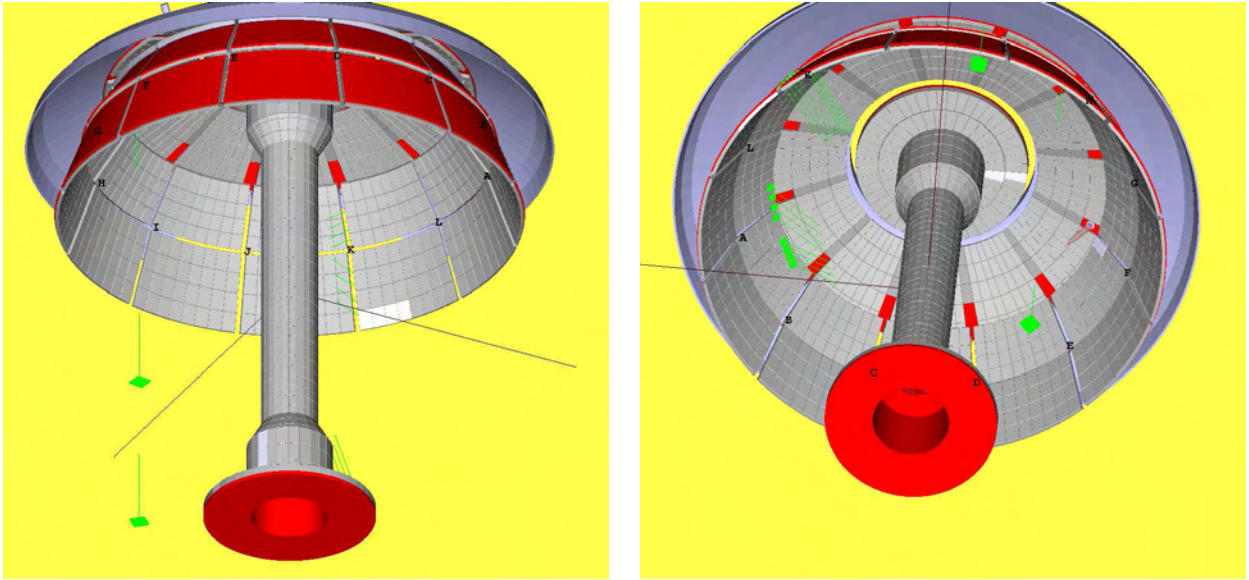
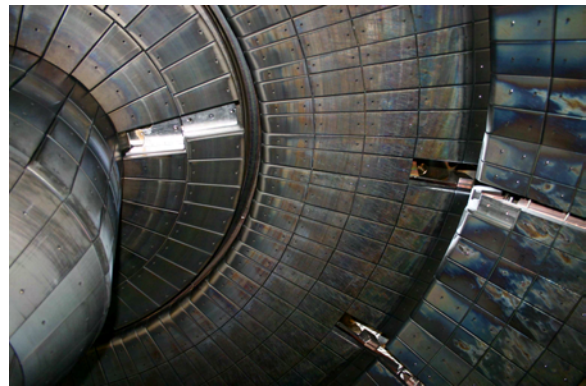


Fig.7. Test tiles in the upper part of the vacuum vessel

Fig.7 shows four test tiles on the upper passive stabilizing plates and two test tile on the upper inner divertor plates.



Test tiles in the K-L sector of the PPP-U plate



Two test tiles in the upper inner divertor region near Bay-F

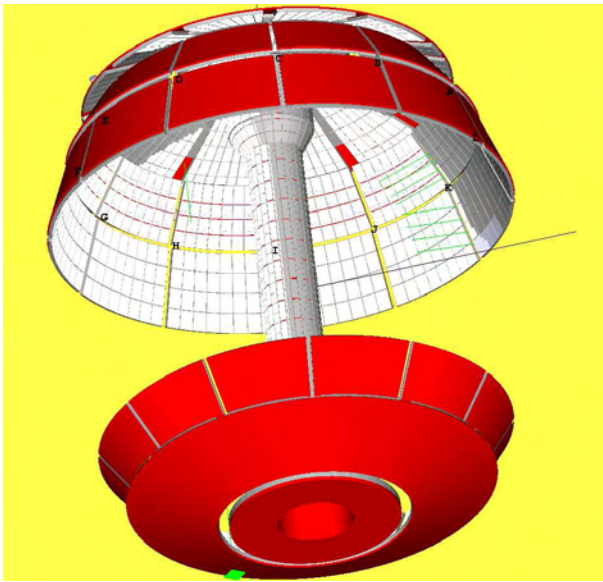
Fig.8 Photographs of test tiles in the upper part of NSTX PFC.

3 Shadow region on the PFC *(to ToC)*

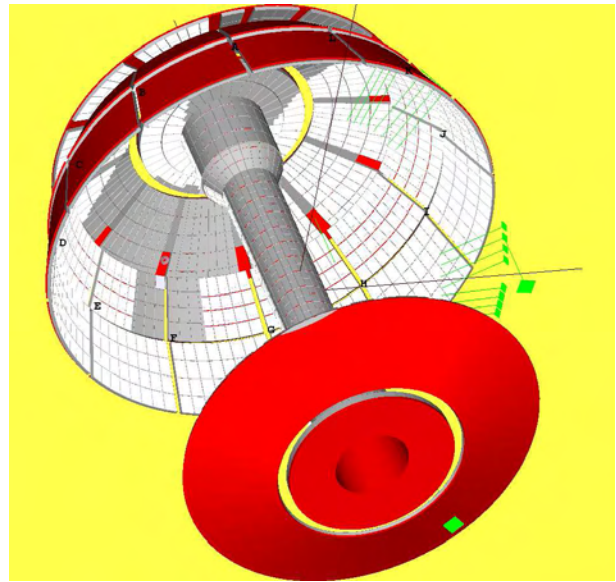
Fig.9 shows the shadow from LITER-1 lithium deposition. *The artificially darker gray columns of tiles on the outer divertor indicate the location of the different Bays, rather than representing a shadow.*

Four test tiles in the lowest row of the left picture (sector K-L) show the transition from the shadow to the exposed region and edge of the shadow.

In the right Fig.9, the front end of the evaporator (gray circle) is visible at the upper edge of the secondary stabilizing plate (Bay F).

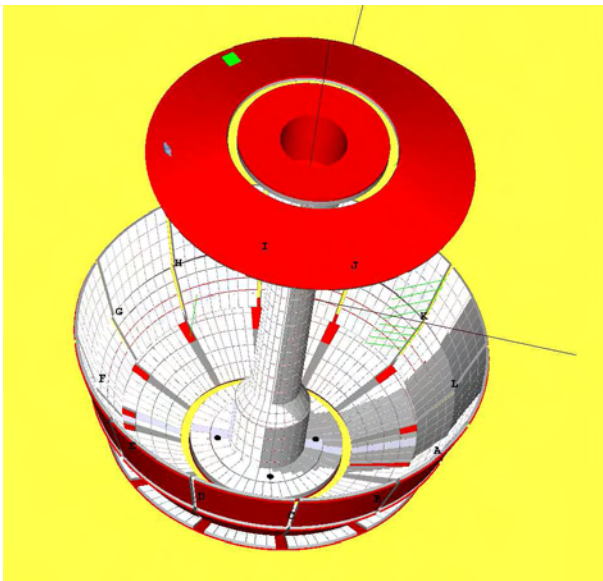


Shadow in the upper K-L sector opposite to LITER-1

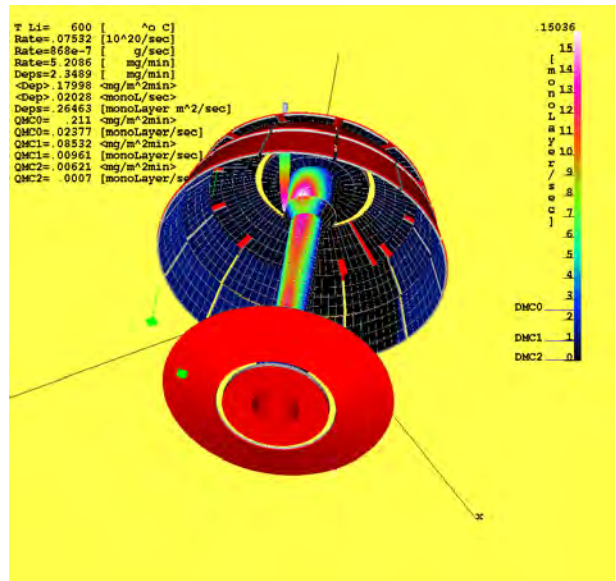


A blind zone near LITER-1 between upper E and H bays

Fig.9 Upper part of NSTX PFC with the Li shadowed regions in gray.



Shadow in the lower K-L in gray



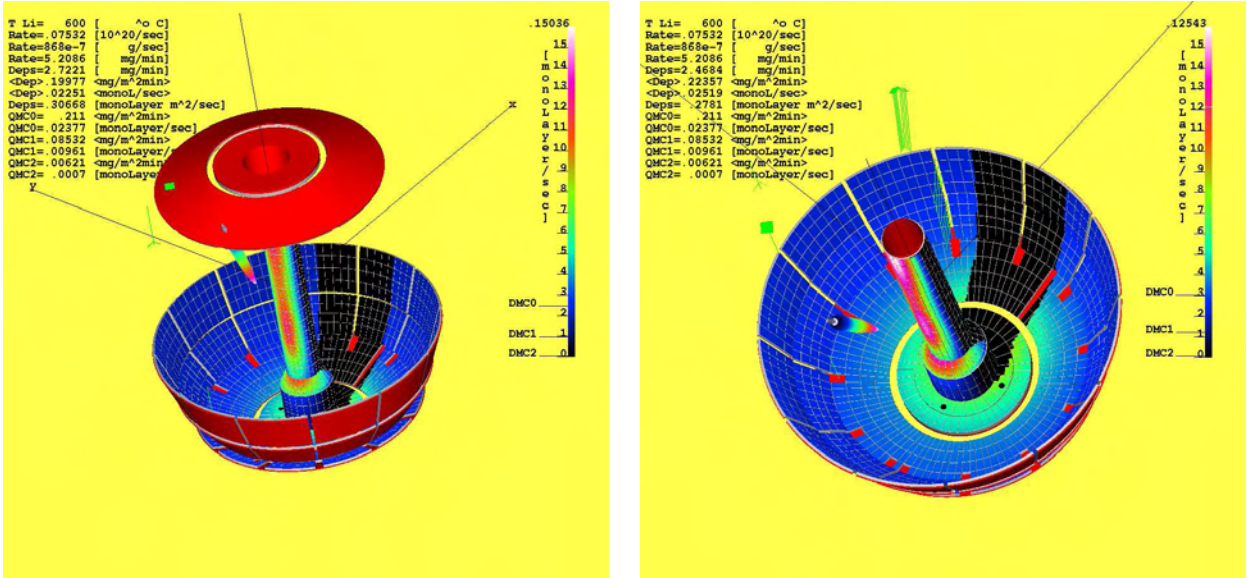
Deposition and the shadow in the upper part of NSTX

Fig.10. Left side shows the shadow in deposition in the lower part of the vacuum chamber. The right side shows the deposition intensity in the upper part of NSTX.

Fig.10 left side shows the lower part of the PFCs with the test tiles in the inner and outer lower divertor in vicinity of Bays L and F.

Fig.10, right side, displays the calculations of the absolute deposition rate of the 600° hot LITER-1 to the upper PFCs shown on the figure. The color rule makes association between the color of the surfaces and the rate of deposition. The number at the top of the color rule corresponds to the maximum rate of deposition on the surface of the displayed PFCs.

Black color here is the shadow (zero rate of deposition).



Deposition rate for lower and upper PFCs

Deposition rate for reduced set of PFCs

Fig.11 Deposition and shadow in the lower K-A sectors.

Fig.11 displays the rate of deposition to the lower part of PFCs. In the right figure the range of the deposition rate scale is calculated based on reduced number of PFC elements in order to increase the contrast between different PFCs.

4 Numerical data for deposition monitors, coupons, and test tiles (to ToC)

The Table 1 of the Appendix list the numerical data on the absolute and relative deposition on the surface of crystal monitors and coupons with respect to the deposition flux Φ_0 to QMB-HL.

The entry Name is the name of the element (see Fig.2) In both tables r, φ, z correspond to cylindrical coordinates r, φ, z with φ counted in its mathematical (counter clockwise) direction with $\varphi = 0$ in the middle of sector 'AL'.

The column $\text{Li}/\text{m}^2\text{sec}$ represents the Li particle flux for 600° C temperature of LITER-1, while gF/gF_0 is the the deposition flux Φ relative to its value Φ_0 on the QMB-HL crystal monitor.

In Table 2, the additional columns have the following meaning: Sect (non empty only for PPP-L,U SPP-L,U) gives the sector label, the columns iT, iR are the tile # in the row #, counted in the directions of φ (Fig.3) and θ (Fig.2) correspondingly.

Additionally, the surface of each test tile is subdivided by 4×4 elements labeled by indexes it, ir, there the first one is counted in the direction of φ and the second one in the direction of θ .

In Table 2 there is no data on the absolute deposition.

Acknowledgment

We wish to acknowledge the technical contributions of NSTX Engineering Staff J. Gething, S. Gifford, and J. Winston. This work is supported by U.S. Department of Energy Contract DE-AC02-76CH03073.

References

- [1] H. W. Kugel *et al.*, Proceedings of 17th Int. Conf. on Plasma Surface Interactions, Heifei, China, May 22-26 , (2006).
- [2] C. H. Skinner *et al.*, Proceedings of 17th Int. Conf. on Plasma Surface Interactions, Heifei, China, May 22-26 , (2006).

5 Appendix *(to ToC)*

Table 1

Deposition on QMB monitors and coupons relative to QMB-HL

#	Name	r[m]	z[m]	gf ^o	T_Li=600^oC Li/(m^2sec)	gF/gF_0	
	gF_0	1.0168	-1.5361	134.76	3.051e+17	1.000e+00	- calibration rate
0	QMB-HL	1.0168	-1.5361	134.76	3.051e+17	1.000e+00	
1	QMB-IM	1.6654	0.1129	97.51	1.619e+17	5.306e-01	
2	QMB-HU	1.0317	1.5488	135.56	8.982e+15	2.944e-02	
3	A	1.2040	1.2526	44.76	1.087e+17	3.563e-01	
4	B	1.2395	1.2020	44.79	1.087e+17	3.561e-01	
5	C	1.2741	1.1526	44.82	1.084e+17	3.552e-01	
6	D	1.3096	1.1017	44.85	1.067e+17	3.498e-01	
7	E	1.4044	0.9048	44.97	1.357e+17	4.449e-01	
8	F	1.4331	0.8175	44.94	1.368e+17	4.483e-01	
9	G	1.4620	0.7298	44.91	1.370e+17	4.490e-01	
10	H	1.4902	0.6439	44.89	1.364e+17	4.471e-01	
11	I	1.4757	-0.6678	45.03	2.078e+17	6.811e-01	
12	J	1.4483	-0.7541	44.99	2.104e+17	6.897e-01	
13	K	1.4206	-0.8415	44.96	2.130e+17	6.980e-01	
14	L	1.3929	-0.9295	44.93	2.157e+17	7.070e-01	
15	M	1.3028	-1.1177	44.89	2.593e+17	8.500e-01	
16	N	1.2664	-1.1687	44.89	2.658e+17	8.713e-01	
17	O	1.2314	-1.2178	44.89	2.738e+17	8.975e-01	
18	P	1.1961	-1.2674	44.91	2.818e+17	9.237e-01	

Table 2, continuation

Name	Sect	iT	iR [it,ir]	r[m]	z[m]	gf ^o	gF/gF_0
OD-L	GF	52	4 [1, 1]	0.9819	-1.4866	189.84	1.074e+00
OD-L	GF	52	4 [1, 2]	1.0094	-1.4757	189.84	1.063e+00
OD-L	GF	52	4 [1, 3]	1.0368	-1.4648	189.84	1.052e+00
OD-L	GF	52	4 [1, 4]	1.0643	-1.4539	189.84	1.040e+00
OD-L	GF	52	4 [2, 1]	0.9819	-1.4866	190.78	1.074e+00
OD-L	GF	52	4 [2, 2]	1.0094	-1.4757	190.78	1.063e+00
OD-L	GF	52	4 [2, 3]	1.0368	-1.4648	190.78	1.052e+00
OD-L	GF	52	4 [2, 4]	1.0643	-1.4539	190.78	1.040e+00
OD-L	GF	52	4 [3, 1]	0.9819	-1.4866	191.72	1.074e+00
OD-L	GF	52	4 [3, 2]	1.0094	-1.4757	191.72	1.063e+00
OD-L	GF	52	4 [3, 3]	1.0368	-1.4648	191.72	1.052e+00
OD-L	GF	52	4 [3, 4]	1.0643	-1.4539	191.72	1.040e+00
OD-L	GF	52	4 [4, 1]	0.9819	-1.4866	192.66	1.074e+00
OD-L	GF	52	4 [4, 2]	1.0094	-1.4757	192.66	1.063e+00
OD-L	GF	52	4 [4, 3]	1.0368	-1.4648	192.66	1.052e+00
OD-L	GF	52	4 [4, 4]	1.0643	-1.4539	192.66	1.040e+00

The Princeton Plasma Physics Laboratory is operated
by Princeton University under contract
with the U.S. Department of Energy.

Information Services
Princeton Plasma Physics Laboratory
P.O. Box 451
Princeton, NJ 08543

Phone: 609-243-2750
Fax: 609-243-2751
e-mail: pppl_info@pppl.gov
Internet Address: <http://www.pppl.gov>